Noise Source Identification in a Cross-Section of a Long-Range Airliner by Means of the Inverse Finite Element Method

M. Weber, T. Kletschkowski, D. Sachau

Helmut-Schmidt-University / University of the Federal Armed Forces, 22043 Hamburg, Germany,
Email: mweber@hsu-hh.de

Introduction

The noise pollution of aircraft cabins results in an unwanted limitation of the passengers comfort, and recurrent exposure to high noise levels can cause serious diseases. In order to reduce the noise exposure of these lightweight structures, passive as well as active methods can be applied.

To achieve a noticeable improvement of the acoustic comfort the interior noise sources have to be identified. This proves to be difficult particularly at frequencies below 500Hz. To localize acoustic hot spots, i.e. the main sources in the structure where sound is transmitted into the cabin, several techniques have been established, ranging from simple sound pressure or intensity measurements to more advanced methods such as Beamforming, Near-Field Acoustical Holography (NAH), Inverse Boundary Element Method (IBEM), or Least-Squares Method (LSM). An up to date overview can be found in [1]. Most of these techniques, however, are either highly ineffective or demand creating artificial free-field conditions to avoid standing waves.

A new approach, based on the Inverse Finite Element Method (IFEM), reconstructs the spatial distribution of sound pressure and particle velocity from pressure measurements taken inside the cabin. This procedure has been validated in 2D and 3D simulation as well as a 2D experiment, see [2, 3, 4, 5, 6].

Inverse Finite Element Method

The FE method for the time-harmonic analysis of interior noise problems is based on the Helmholtz equation

$$\Delta p(\mathbf{x}) + k^2 p(\mathbf{x}) = 0\,, \tag{1}$$

where Δ represents the Laplace operator and $k = 2\pi f / c$ the wave number that is determined by the excitation frequency f and the speed of sound c. The corresponding boundary conditions (BC) are given by the Dirichlet BC for the acoustic pressure

$$p = \overline{p} \quad \text{on } R_p\,, \tag{2}$$

and the Neumann BC for the normal component of particle velocity

$$-\mathbf{n}\cdot\frac{1}{\rho}\nabla p = i(2\pi f)\overline{v}_n \quad \text{on } R_v\,. \tag{3}$$

Discretization of Eq. (1) using the FE method leads to a set of algebraic equations for the sound pressure that can be summarized as

$$\mathbf{K}\mathbf{p} = \mathbf{v}\,. \tag{4}$$

$\mathbf{K}$ is the stiffness matrix, $\mathbf{p}$ the vector of the excess pressure and $\mathbf{v}$ a vector that is proportional to the particle velocity in the sound field, and therefore called generalized velocity vector. The solution of Eq. (4) with respect to the BC leads to the unknown pressure field $\mathbf{p}$. This process is called forward calculation.

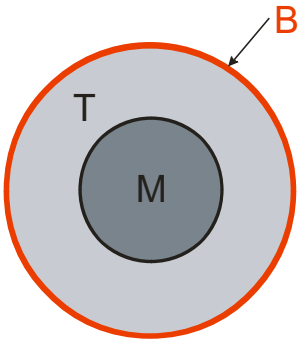

Figure 1: The calculation domain is split into three regions: M, T and B.

In order to derive the IFEM the calculation domain is split into three regions: an inner measurement sub-domain (M), a transition sub-domain (T), and an outer boundary (B) as illustrated in Figure 1. It is possible to decompose Eq. (4) as follows:

$$\begin{bmatrix} \mathbf{K}_1 & \mathbf{K}_2 & \mathbf{K}_3 \\ \mathbf{K}_4 & \mathbf{K}_5 & \mathbf{K}_6 \\ \mathbf{K}_7 & \mathbf{K}_8 & \mathbf{K}_9 \end{bmatrix} \begin{bmatrix} \mathbf{p}_{MK} \\ \mathbf{p}_{TU} \\ \mathbf{p}_{BU} \end{bmatrix} = \begin{bmatrix} \mathbf{v}_{MK} \\ \mathbf{v}_{TK} \\ \mathbf{v}_{BU} \end{bmatrix}. \tag{5}$$

The first index of the three sound pressure sub-matrices $\mathbf{p}_{ij}$ and the three sub-matrices $\mathbf{v}_{ij}$ of the generalized velocity vector $\mathbf{v}$ denotes the sub-domain of the decomposed calculation domain, whereas the second index denotes whether the variable is known (K) or unknown (U).
As described in [4], in the absence of unknown volume sources in the transition and measurement sub-domain the unknown parts of the sound pressure vector $\mathbf{p}$ can be computed by the solution of a reduced problem that is given by

$$\begin{bmatrix} \mathbf{K}_2 & \mathbf{K}_3 \\ \mathbf{K}_5 & \mathbf{K}_6 \end{bmatrix} \begin{bmatrix} \mathbf{p}_{TU} \\ \mathbf{p}_{BU} \end{bmatrix} = \begin{bmatrix} -\mathbf{K}_1\,\mathbf{p}_{MK} \\ -\mathbf{K}_4\,\mathbf{p}_{MK} \end{bmatrix} \tag{6}$$

and

$$\begin{bmatrix}\mathbf{K}_8 & \mathbf{K}_9 & -\mathbf{I}\end{bmatrix}\begin{bmatrix}\mathbf{p}_{TU}\\ \mathbf{p}_{BU}\\ \mathbf{v}_{BU}\end{bmatrix}=\begin{bmatrix}-\mathbf{K}_7\,\mathbf{p}_{MK}\end{bmatrix}. \qquad (7)$$

Eq. (7) leads to the unknown velocities at the outer boundary. This procedure is called inverse calculation.
Eq. (6) must be solved to determine the complete sound field in the interior using only the measurements in the inner region of the sound field. For simplicity it is rewritten as follows:

$$\mathbf{Ax} = \mathbf{b}\,; \qquad (8)$$

$$\mathbf{A} \equiv \begin{bmatrix}\mathbf{K}_2 & \mathbf{K}_3\\ \mathbf{K}_5 & \mathbf{K}_6\end{bmatrix}, \mathbf{x} \equiv \begin{bmatrix}\mathbf{p}_{TU}\\ \mathbf{p}_{BU}\end{bmatrix}, \mathbf{b} \equiv \begin{bmatrix}-\mathbf{K}_1\,\mathbf{p}_{MK}\\ -\mathbf{K}_4\,\mathbf{p}_{MK}\end{bmatrix}.$$

As stated in [2] it has been found that the condition number of the new portioned stiffness matrix **A** is very high, especially if realistic measurement errors are taken into account. Therefore, several regularization techniques such as Truncated Singular Value Decomposition (TSVD), Tikhonov Regularization (TR) or Conjugated Gradient Least Squares (CGLS) have been applied to solve the ill-posed problem that is given by Eq. (8). Details about the application of these regularization algorithms have been reported in [4].

Application of the IFEM in an Aircraft Mock-Up without Seats

Mapping of the Mock-Up

In a first validation step, the sound field inside a special acoustic mock-up for a long range aircraft cabin is measured for a defined source location. The mock-up is fully equipped with lining, floor and hat racks; the seats have been removed. The ends are closed with absorbing foam wedges. It is excited by a loudspeaker located in one corner of the fuselage section. The measured sound pressure values are assigned to the mesh nodes of a matching FE model of the cavity. Thus, the inner sub-domain is defined by the full extent of the mapped area. Figure 2 shows the mock-up and the acoustic model of the cabin. Details about the mapping procedure can be read in [7].

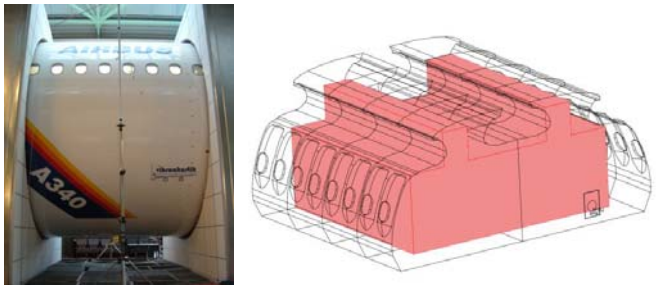

Figure 2: Mock-up and matching acoustic model of the cabin. The coloured volume marks the inner sub-domain where pressure measurements are taken.

Results of the Inverse Calculation

The pressure values measured at positions located inside the inner sub-domain are linearly interpolated to the mesh points. Figure 3a shows the normal acceleration calculated by the IFEM on the boundary plane containing the internal loudspeaker (left), and on the plane opposite to it (right), for f = 90Hz. The reconstruction of the loudspeaker location is nearly exact. For this calculation, a coarse mesh containing approx. 27,000 DOF performs best. The CGLS regularization technique used here, an iterative algorithm, is most feasible for large-scale problems. The optimal regularization parameter, i.e. the number of iterations, determined via the NCP ("Normalized Cumulative Periodogram") method, is γ = 55.

The NCP method takes advantage of the fact that solutions of non-regularized, ill-posed problems tend to show strong spatial oscillations. This leads to a high amount of noise in terms of high spatial frequencies in the residual vector **e** = **Ax** – **b**. On the other hand, over-regularized solutions are highly incorrect, so that the residual vector is dominated by the low-frequent signal part. The optimal regularization parameter is estimated by finding the number of iterations where the residual spectrum comes closest to white noise.

This method is well-suited for large-scaled problems (see [8]). However, to fully exploit the physics of the problem, it would be necessary to resort the (one-dimensional) residual vector to a (two-dimensional) matrix that represents the actual adjacency of the nodes before performing a FFT. For this reason, the NCP algorithm implemented here cannot be applied for all mesh configurations and needs further improvement.

Figure 3b shows the same calculation for f = 200Hz, with slightly different parameters. Here, a finer mesh containing approx. 69,000 DOFS is used; an optimal regularization parameter γ = 27 is determined via the L-Curve method that finds a trade-off between error norm and solution norm (see [9]). Again, the sound source is located. However, whereas at f = 90Hz the foam wedges appear to represent a sound-hard termination, they seem to absorb at f = 200Hz. This is confirmed by displaying the real-valued intensity, as shown in Figure 3c. Considering the outward pointing normal vector of the plane, the loudspeaker appears as a source, and the foam wedges opposite to it appear as sinks.

As for a quantitative evaluation of the results, the acceleration values calculated at the loudspeaker position are compared to those measured on the loudspeaker membrane. For both frequencies considered, the computed values are about one tenth of the measured values. This could be due to the fact that the calculated "loudspeaker" appears blurred compared to the real membrane. Also, for mechanical reasons, the distance between measurement area and wall is rather large (approx. 0.7m). A smaller distance could still improve this result.

a) f = 90Hz: Magnitude of normal acceleration (m/s^2)

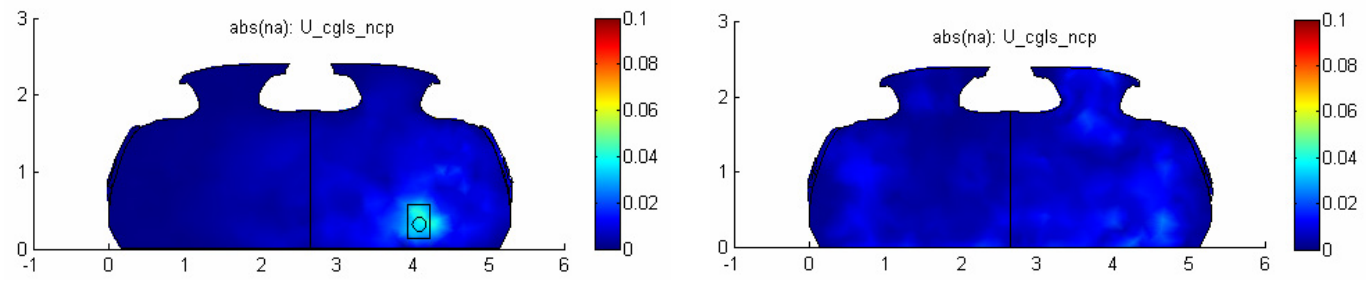

b) f = 200Hz: Magnitude of normal acceleration (m/s^2)

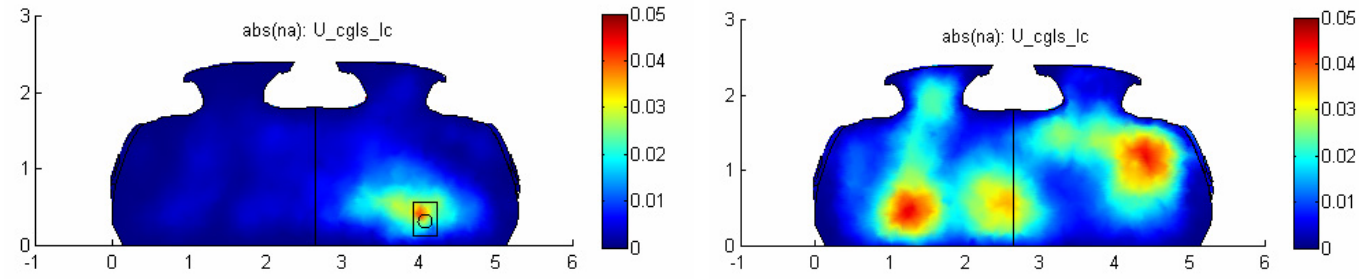

c) f = 200Hz: Normal intensity (Pa m/s^2)

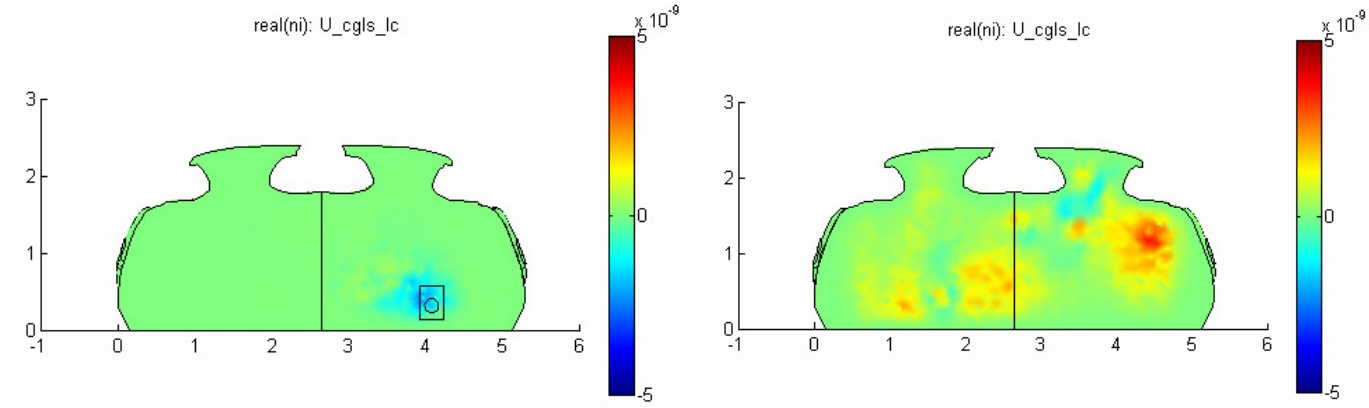

Figure 3: Normal acceleration for f = 90Hz and f = 200Hz, normal intensity for f = 200Hz. Left: "front" boundary plane showing position of loudspeaker; right: "back" boundary plane.

Application of the IFEM in an Aircraft Mock-Up Including Seats

Mapping of the Mock-Up

In a second step, the mapping procedure is repeated with built-in seats, while the space between the backrests of the seats remains unmapped (see Figure 4). Thus, the extent of the measurement sub-domain is much smaller in relation to the whole cavity than before, which results in a highly under-determined equation system. Instead of a speaker, now a Volume Velocity Source (VVS) is used for excitation. This has the advantage that it provides an exact value for particle velocity at the well-defined orifice of the source, which can be used for quantitative validation of the IFEM. For further validation, certain areas located on the lining, the floor, the foam wedges and the hat rack are mapped with acceleration sensor arrays and a sound intensity probe.

In addition, two further mapping procedures are performed: next, the VVS is replaced by a loudspeaker positioned inside the hat rack. Finally, the cavity is excited by two exterior loudspeakers placed at locations where the engines would be. Again, validation data is recorded. However, the analysis of these mapping procedures is still subject to present work. The following statements are limited to the first mapping with VVS excitation.

Details about the mapping procedure can be read in [7].

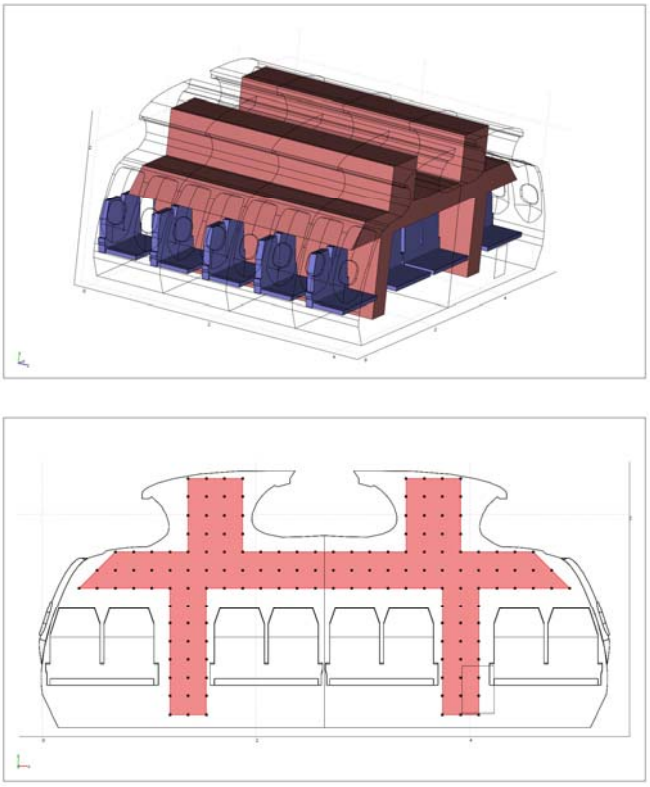

Figure 4: FE model containing seats and measurement sub-domain. The lower slice plot also shows the measurement grid.

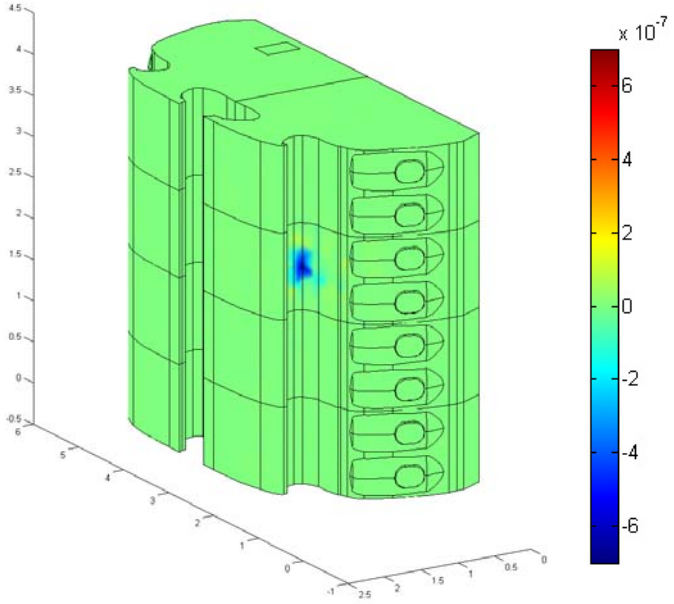

Figure 5: Normal intensity (Pa m/s^2) on the boundary calculated by the IFEM (f = 200Hz). The position of the source is clearly visible.

Results of the Inverse Calculation

Figure 5 shows the result of the IFEM, exemplarily performed for f = 200Hz. A coarse mesh containing approx. 23,000 DOFS is used here; the factor of under-determinedness is approx. $k = 0.6$ (as opposed to $k > 1$ for an over-determined system). An optimal CGLS regularization parameter $\gamma = 211$ is determined via the L-Curve method. In consideration of the normal intensity on the boundary, the location of the sound source is exactly reconstructed. This plot looks similar for several frequencies examined between 50Hz and 800Hz. At present no statement can be made on the quantitative validation of this calculation, as the reference data have not been interpreted so far.

Outlook

Present work deals with the quantitative validation of the calculation results, covering both internal (VVS, loudspeaker) and external sources. In upcoming research, the IFEM technique will have to be stabilized and made numerically more efficient. Moreover, sensitivity studies concerning the reduction of measurement data will be performed to make the method more applicable.

References

[1] S. F. Wu, “Methods for reconstructing acoustic quantities based on acoustic pressure measurements”, The Journal of the Acoustical Society of America (2008) 124 (5): 2680 - 2697

[2] J. Drenckhan, D. Sachau, “Identification of sound sources using inverse FEM”, Proceedings of the 11th Int. Congress on Sound and Vibration, Stockholm (2003)

[3] J. Drenckhan, D. Sachau, “Identification of sound sources using inverse FEM”, 7th Int. Symposium “Transport Noise and Vibration“, St. Petersburg (2004)

[4] D. Sachau, J. Drenckhan, T. Kletschkowski, S. Petersen, “Entwicklung von Messtechniken zur Lärmquellenidentifizierung in Kabinen“, Final report LUFO HH TUT-34, Helmut Schmidt University Hamburg (2005)

[5] M. Weber, T. Kletschkowski, D. Sachau, „Identifikation von Schallquellen mittels inverser FEM mit realen Messdaten“, DAGA’08, Dresden

[6] M. Weber, T. Kletschkowski, D. Sachau, “Identification of noise sources by means of inverse finite element method using measured data”, Acoustics’08, Paris

[7] K. Simanowski, T. Kletschkowski, D. Sachau, B. Samtleben, “Acoustic Ground Tests in a Cross-Section of a Long-Range Airliner for Validation of the Inverse Finite Element Method”, NAG/DAGA’09, Rotterdam

[8] P. C. Hansen, M. E. Kilmer, R. H. Kjeldsen, “Exploiting Residual Information in the Parameter Choice for Discrete Ill-Posed Problems“, BIT Numerical Mathematics (2006) 46: 41-59, Springer

[9] P. C. Hansen, “Rank-Deficient and Discrete Ill-Posed Problems”, Vol. 1, Society for Industrial and Applied Mathematics, Philadelphia (1998)